An All-Digital 1.25 Mbps 5-Subcarrier OFDM Backscatter Uplink with Delta-Sigma Modulation for Improved Spurious-Free Dynamic Range

James D. Rosenthal[1] and Matthew S. Reynolds[2]
School of Engineering (STI)[1]
Swiss Federal Institute of Technology (EPFL)
Lausanne, Switzerland
Department of Electrical & Computer Engineering[2]
University of Washington
Seattle, WA, USA
jamesdrosenthal@ieee.org[1]

***Abstract*— This paper describes an all-digital backscatter modulation approach leveraging delta-sigma modulation (DSM) to improve the in-channel spectral characteristics of orthogonal frequency division multiplexed (OFDM) backscatter communication. We demonstrate through numerical simulations and experimental validation that DSM can improve the spurious-free dynamic range (SFDR) of OFDM subcarriers generated by a low-resolution impedance digital-to-analog converter (DAC), such as an RF switch having two or four different impedance states. We present the design and validation of a prototype OFDM backscatter uplink with DSM implemented with all-digital logic in an FPGA. A single-pole-four-throw CMOS RF switch (i.e. 2-bits of impedance DAC resolution) serves as the backscatter modulator. We experimentally validated the DSM approach with a 2.4 GHz, five-subcarrier OFDM backscatter uplink and a four-times oversampling DSM at up to 1.25 Mbps. In this scenario, the DSM improved the SFDR by 4.3 dB within the subcarrier band while reducing the overall noise floor in the same band by 11.3 dB. These results confirm that a DSM approach can be used to control quantization noise and improve the spectral characteristics of low-resolution digital impedance modulators for backscatter communication in scenarios where in-channel SFDR is more important than wideband noise performance.**

***Keywords*— backscatter communication, delta-sigma modulation, OFDM.**

I. Introduction

Ultra-low power backscatter communication enables wireless data uplinks having orders of magnitude lower energy consumption per data bit transferred, compared to conventional wireless links such as Bluetooth Low Energy and Wi-Fi. Most existing backscatter communication systems have relied on single-carrier modulation in order to uplink data [1]. Two major drawbacks to single-carrier backscatter modulation are higher sensitivity to multipath interference and limited flexibility for multiple access schemes. In contrast, multi-carrier modulations, such as orthogonal frequency division multiplexing (OFDM) (Fig. 1), can provide greater robustness to multipath fading while additionally providing more flexibility for multiple access schemes. This has made OFDM backscatter an appealing modality using both mixed-signal [2], [3] and all-digital architectures [4], [5].

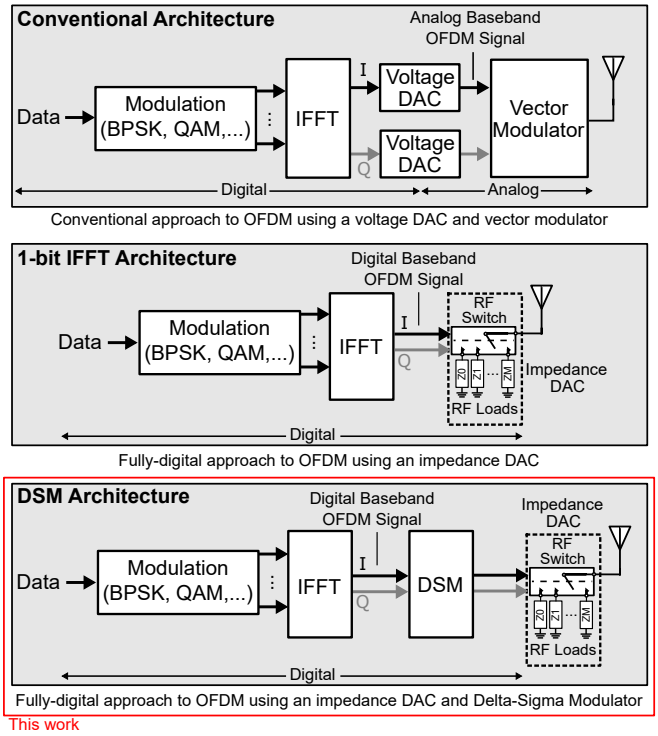

Fig. 1. Conventional OFDM architectures (top) rely on power hungry analog electronics like voltage digital-to-analog converters (DACs) and vector modulators. In this work, we compare the performance of two all-digital architecture for OFDM backscatter communication: a 1-bit IFFT version from [4] (middle) and a delta-sigma modulator (DSM) approach presented here for the first time (bottom).

All-digital OFDM backscatter communication, as shown in Fig. 1, has recently been demonstrated using low-complexity and low-power single-bit or two-bit digital impedance modulators [4]. A consequence of using low-resolution switched impedance modulators, though, is an elevated noise

https://doi.org/10.1109/RFID54732.2022.9795980

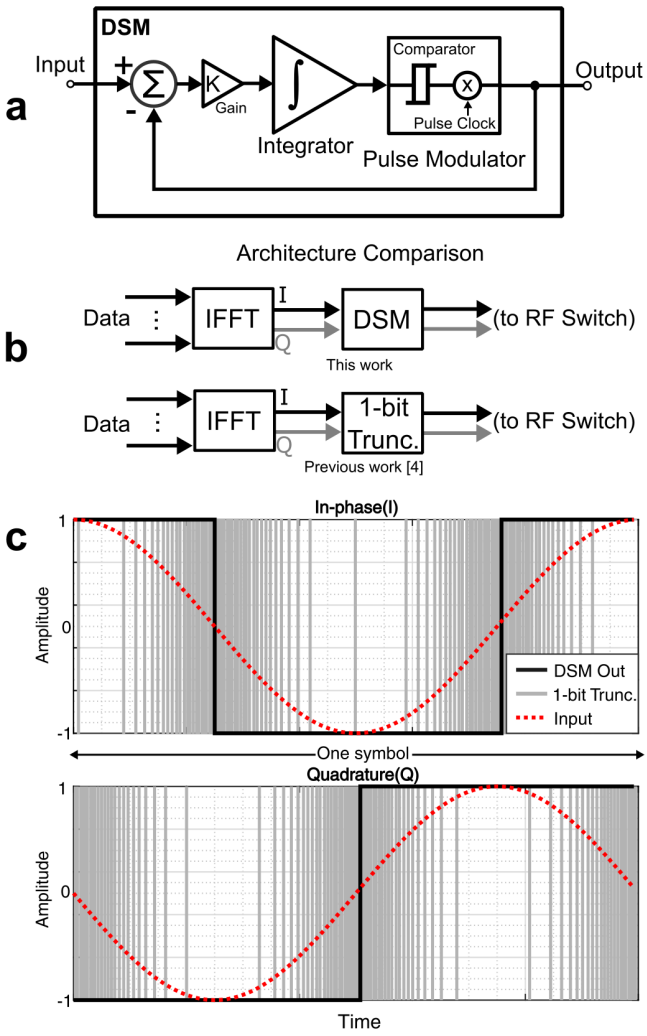

Fig. 2. This work uses a delta-sigma modulator (DSM) similar to the architecture in (a) to encode the time-domain IFFT output (b). The full-resolution IFFT result (*Input*), a truncated 1-bit version of the IFFT result (*1-bit Trunc.*), and the DSM output are plotted for comparison (c).

floor due to increased quantization noise from the lower resolution signal representation. The elevated noise floor degrades the spurious-free dynamic range (SFDR) of the OFDM subcarriers, limiting the signal-to-noise ratio in the received channel.

In this work, we present an new architecture for all-digital OFDM backscatter that improves the SFDR by using delta-sigma modulation (DSM) (Fig. 1). In prior work, DSM has been shown to leverage oversampling to increase the effective resolution of voltage digital-to-analog converters (DACs) [6]. In this work, we extend the DSM concept to include impedance DACs that function as backscatter modulators. A DSM encodes the changes of a multi-bit input signal as an over-sampled series of one-bit pulses. A common DSM architecture is shown in Fig. 2(a). By feeding back and subtracting the output pulses, DSMs reduce the effective quantization error. In the frequency domain, this has the effect

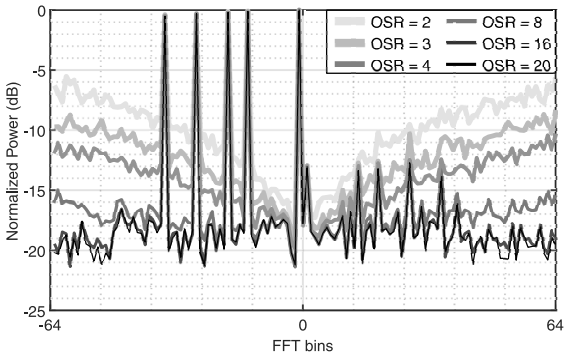

Fig. 3. Plot showing the FFT calculated for the DSM signal generated using different oversampling ratios (OSRs).

of shaping the noise, resulting in lower noise below the input signal's Nyquist frequency.

DSM has previously been investigated for a single-carrier, offset-frequency QAM backscatter transponder [5]. The authors provided analysis and simulation results to demonstrate improvements to single-carrier modulation for compatibility with IEEE 802.11 standards. In this work we provide hardware design detail, analysis, and performance measurements of an all-digital OFDM backscatter uplink that employs DSM to reduce quantization noise in the channel. To the best of our knowledge, this is the first presentation and the first hardware validation of such a multi-carrier backscatter uplink concept. In Section II, an overview of the design is provided, including characterization of the backscatter modulator, the backscattered power spectrum, and the data uplink. Section III provides conclusions from these measurements and suggestions for future work.

II. Design Overview & Characterization

The OFDM backscatter uplink presented in this work uses delta-sigma modulation (DSM) to reduce low-frequency quantization noise in the vicinity of modulated subcarrier tones. The DSM is based on a classic architecture illustrated in Fig. 2(a) [7] and operates on multiple subcarriers present at the output of the IFFT, as shown in Fig. 1 and Fig. 2(b). This architecture is different from a previously published OFDM backscatter modulator presented in [4] that truncated the IFFT outputs to the most significant bit (MSbit), as shown in Fig 1. In this implementation, high resolution (e.g. 16-bit) in-phase (I) and quadrature (Q) signals from the IFFT are input to the DSM where they are converted into an over-sampled pulse train with 1-bit amplitude. The DSM performance can be altered by changing the gain, the comparator threshold, and the oversampling rate (OSR). Example plots of the input and output signals of the DSM for one OFDM symbol are shown in Fig. 2(c). The truncated IFFT results (*1-bit Trunc.*) are plotted as well for comparison. The data used in these plots corresponds to one subcarrier using single sideband (SSB) modulation, resulting in a complex IFFT output signal. A gain of 4, threshold of 0, and an over-sample rate of 4 are used.

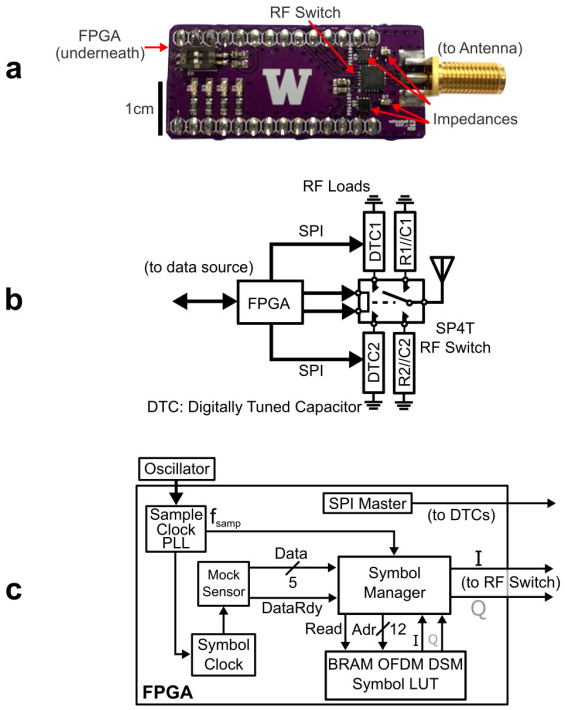

Fig. 4. The hardware test board is implemented using off-the-shelf parts and custom logic implementetd with Verilog HDL. (a) Photo of the PCB with an RF switch and RF impedances (DTCs and resistor/capacitor pairs) [4], [8], (b) Block diagram of the PCB components [4], [8], (c) Block diagram of the FPGA-based digital logic using a look-up table (LUT) for the OFDM DSM symbols.

A. *Effect of the Oversampling Ratio (OSR)*

A critical parameter for DSMs is the OSR, which directly affects quantization noise of the modulated signal. For example, increasing the OSR by a factor of four theoretically yields a 6-dB reduction in quantization noise for a full-scale sinusoidal input. This 6-dB improvement is equivalent to adding one effective bit to the converter [6]. While using a higher OSR reduces the quantization noise, it also requires using a faster system clock and, in the case of the LUT-based architecture used in this work (Fig. 1), more memory. Simulations were performed in Matlab (Mathworks) to analyze how quantization noise changed with OSR. OFDM signals with five BPSK-modulated subcarriers were generated using a 128-point IFFT and passed through a DSM with a gain of 4, comparator threshold of 0, and variable OSR. The FFT was then performed on the symbols output from the DSM, as shown in Fig. 3.

The FFT output revealed that as the OSR increases, the total noise power decreases within the vicinity of the subcarriers. The reduction in noise power appears to begin saturating at an OSR of 8, with diminishing reductions in noise power for higher OSRs. Based on these simulations, an OSR of 4 was selected for the hardware implementation, because it presented a significant reduction in the noise power while also requiring only four times the memory of the 1-bit truncated design in [4].

Table 1. Resource allocation for the 1-bit Truncated OFDM and DSM OFDM architectures employing five subcarriers

Architecture	f_{samp}	Logic Cells	Multipliers	BRAM (kB)
1-bit Trunc.	32 MHz	663	0	2
DSM	128 MHz	693	0	4

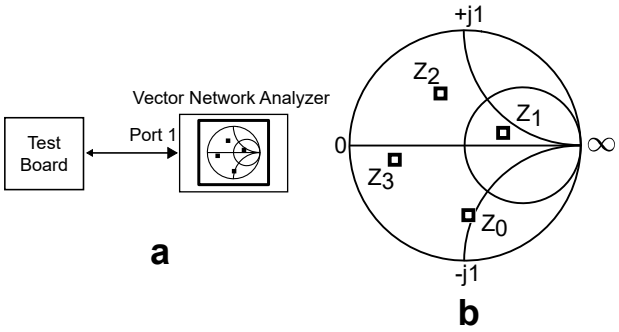

Fig. 5. The reflection coefficients of the backscatter modulator impedance states were measured using a vector network analyzer (a), yielding a four-state impedance constellation plotted on Smith Chart (b).

B. *Hardware Implementation*

The design is implemented using off-the-shelf components and a custom, low-cost FR-4 printed circuit board (PCB) to integrate the backscatter modulator and test circuitry (Fig. 4(a)). The backscatter modulator consists of an Analog Devices ADG904 RF switch, two digitally-tuned capacitors (DTCs) (Peregrine Semiconductor), and two pairs of discrete lumped elements, as shown in Fig. 4(b). The ADG904 was chosen because it provides fast switching times ($\sim$10 ns), four poles for SSB modulation, invariance to external RF power levels relative to e.g. transistor-based modulators [8], and µW power consumption. The digital logic is implemented on a TinyFPGA BX which uses a Lattice Semiconductor iCE40 FPGA. The logic modules were written in Verilog HDL and are illustraed the block diagram of Fig. 4(c).

The digital logic uses a look-up table (LUT)-based architecture for transmitting OFDM DSM backscatter symbols. As is discussed in [4], a LUT-based architecture can be a hardware-efficient method for OFDM backscatter designs that use a low number of a subcarriers. The logic resources needed for the DSM and 1-bit truncation designs are listed in Table 1. For a system using N single sideband (SSB) subcarriers with M-ary modulation, there are M^N symbols for the in-phase (I) channel and M^N symbols for the quadrature channel (Q), yielding $2 * M^N$ total symbols to be stored in the LUT. In this work we use $N = 5$ SSB subcarriers with $M = 2$ binary phase-shift keying (BPSK) modulation, yielding $2 * 2^5 = 64$ total LUT entries. The LUT entries were pre-generated using a Matlab script that calculated the 128-point IFFT outputs for all possible data inputs before passing the output through a DSM. Using an over-sample rate of 4, the script generated a 32 x 512 matrix for both the in-phase and quadrature symbols. The resulting matrices are initialized on block random access memory (BRAM) on the FPGA.

Table 2. Backscatter modulator impedances designed for a carrier frequency of 2.45 GHz

Z	Impedance States R Value	C Value	Γ	DTC Word
Z_0	-	2.5 pF	0.02 - j0.70	0x02
Z_1	-	1.45 pF	0.41 + j0.10	0x08
Z_2	131 Ω	0.5 pF	-0.21 + j0.46	-
Z_3	19.1 Ω	0.5 pF	0.61 + j0.12	-

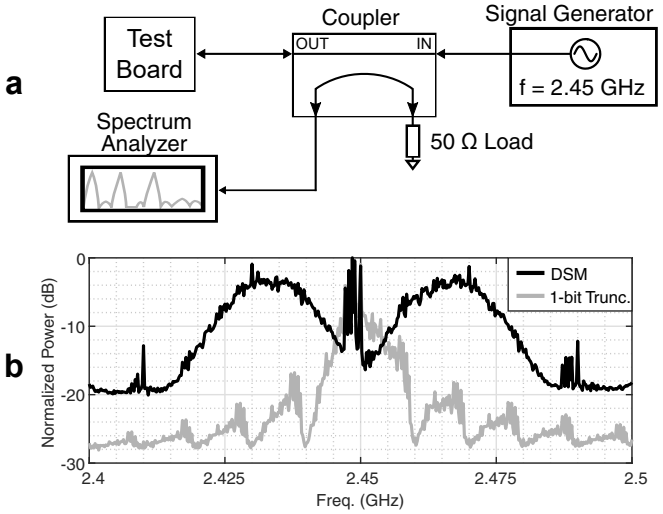

Fig. 6. The backscattered spectra of IFFT 1-bit OFDM [4] and the DSM OFDM designs were compared: (a) Block diagram of the cabled measurement setup, (b) A zoomed-out plot of the spectra demonstrating the noise shaping characteristics of the DSM design

Sensor data is simulated within the FPGA using both a linear feedback shift register (LFSR) to generate pseudo-random bit sequences and a sinewave LUT. Data is output from the "Mock Sensor" logic at a rate set by the symbol clock. As new data bits are generated at each symbol clock, the Symbol Manager module generates a read address and fetches the corresponding time-domain sequence from the BRAM OFDM DSM Symbol LUT. The I and Q symbols are then shifted out as control signals for the RF switch.

C. Impedance Constellation

To ensure optimal sideband suppression, the impedance values for the backscatter modulator were calculated to yield reflection states with equal magnitudes and evenly spaced phases [9], [10], [4]. A vector network analyzer (VNA) was used to measure the complex reflection coefficient of each impedance relative to 50 Ω, as shown in Fig. 5. The DTCs were then iteratively tuned until the optimal magnitude and phase angles of the reflection coefficients were achieved. A summary of the impedances, the measured reflection coefficients, and the DTC tuning words is provided in Table 2.

D. Backscattered Spectrum

To characterize the noise shaping characteristics of the DSM, the backscattered power spectral density was measured using the test setup in Fig. 6(a). An Agilent N5181A RF signal generator set to 2.45 GHz was connected to the test board from Fig. 4 via a Mini-Circuits ZABDC20-252H-S+ directional coupler. The backscattered spectrum was then measured at the output coupled port with an Agilent N9320B spectrum analyzer. The resolution bandwidth was set to 1 kHz over a 100 MHz frequency span and averaging was enabled over 10 sweeps. The test board was programmed for two configurations: (1) using the 1-bit truncated IFFT as in [4] with sample frequency f_s, and (2) using the DSM with sample frequency $4 * f_s$. Both designs were configured to transmit five SSB OFDM subcarriers. A plot of the normalized power spectra is shown in Fig. 6(b), demonstrating how the DSM increases the out-of-channel noise while reducing the low-frequency noise in-channel, in the vicinity of the subcarriers. An analysis of the noise within the subcarrier frequency band is presented in Section. II-F.

E. Data Uplink

The complete signal chain of the OFDM design using DSM was validated using a software-defined radio (SDR) receiver (Ettus Research, USRP B210) to down convert and demodulate the transmitted data. The cabled test setup shown in Fig. 7(a) was used for the measurements. Five subcarriers were used at 62.5 kHz, 875 kHz, 1.19 MHz, 1.69 MHz, and 2.19 MHz. The receiver shown in Fig. 7(b) was implemented in GNU Radio Companion and based off a previous design presented in [11]. The receiver processing flow consists of a down converter to generate the baseband I/Q samples, a poly-phase clock filter to synchronize the sample clock, a Costas Loop to perform phase alignment, and I/Q demodulation to yield the I/Q time-domain sequences. The demodulated I/Q signals are then post-processed in Matlab, where the start of frame (SOF) is identified using correlation, symbols are de-interleaved, and an FFT performed for phase demodulation of the subcarriers.

Tests were run by transmitting pre-calculated sinewave samples from memory, depicted as *Mock Sensor* in Fig. 4(c). As shown in Fig. 7(c), the received backscattered symbols show good agreement with the ideal constellation, yielding an error vector magnitude of 11.66 %. The subcarriers were then demodulated in Matlab, with a plot of the individual subcarrier BPSK constellations shown in Fig. 7(d). From the subcarriers, the data could be demodulated and reconstructed. A plot of the received data in Fig. 8 displays good agreement between the received and original waveforms. No bit errors were detected over several seconds of recorded data.

F. Spectral Improvement Using DSM

OFDM backscatter transmissions using DSM and 1-bit IFFT truncation were compared using the FFT of received data symbols. Each design was configured to transmit 10,000 pseudo-random data symbols (50,000 bits) from an LFSR using 5-subcarrier OFDM backscatter. The backscattered transmissions were then processed using the test setups in Fig. 7(a) and (b). At the output of the FFT, the DSM spectrum exhibits a lower noise floor and less spurious power between subcarriers compared to the 1-bit truncation design. To quantify the improvement, the spurious free dynamic range

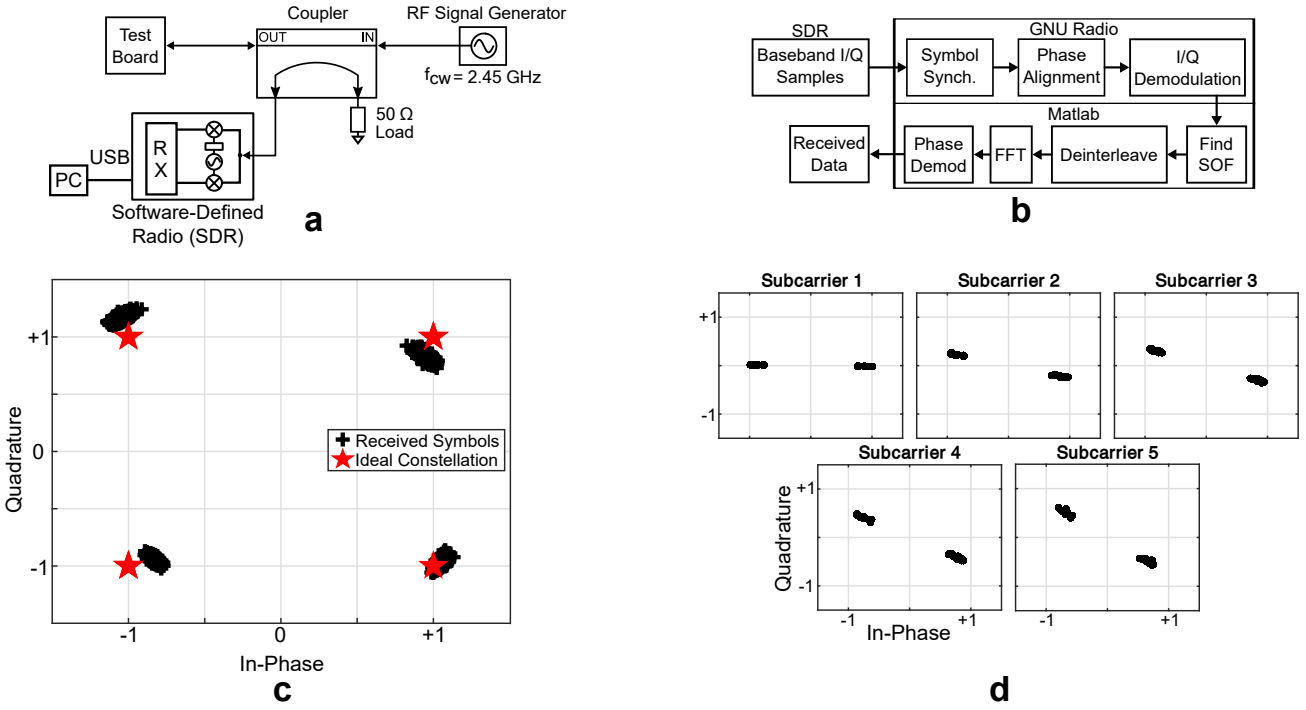

Fig. 7. Data transfer was tested using the DSM OFDM backscatter system: (a) Block diagram of the measurement setup using a software-defined radio as the receiver, (b) Block diagram of the receiver processing flow, (c) Comparison of the received and ideal symbol constellations at the output of the *Phase Alignment* block in GNU Radio, (d) Plot of the modulated subcarrier constellations for 10k symbols at the output of the *FFT* block in Matlab.

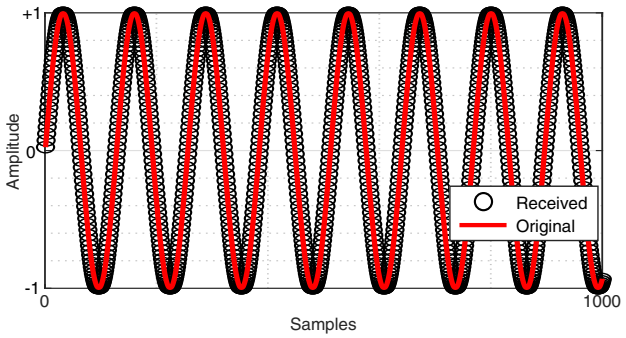

Fig. 8. Plot of the received data samples showing good agreement with the original transmitted sinusoidal signal. No data drops were detected.

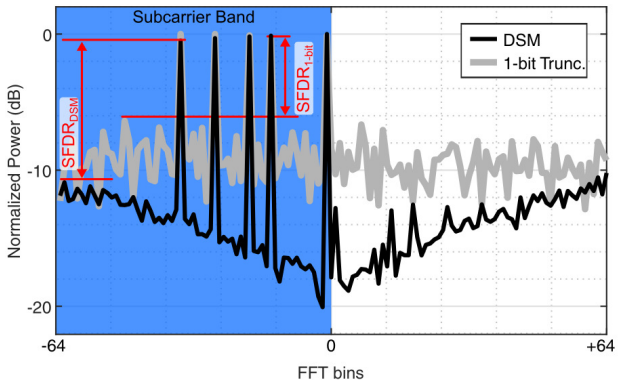

Fig. 9. Comparison of the the IFFT 1-bit and DSM spectra at the output of the receiver FFT. The spurious-free dynamic range (SFDR) is improved for the DSM design within the shaded subcarrier band.

(SFDR) was calculated within the subcarrier band. For this work, we define the SFDR as the ratio between weakest subcarrier power and the largest noise or harmonic distortion component within the smallest frequency band containing all the subcarriers:

$$\text{SFDR} = \text{Power of the weakest subcarrier (dB)} - \text{Power of the strongest spur (dB)}. \quad (1)$$

Based on this definition, the SFDR was calculated for both designs, as depicted in Fig. 9. The SFDR was found to be 12.4 dB for the DSM design and 6.6 dB for the 1-bit truncation design, yielding a 5.8 dB improvement in the SFDR across the subcarrier band. Next, the noise power within the subcarrier band was calculated by summing the power in all FFT bins except those corresponding to a subcarrier. It was found that the total noise power within the subcarrier band was also reduced by 13.2 dB.

III. Conclusions & Future Work

This work presents an all-digital architecture for improving the spurious-free dynamic range of orthogonal frequency division multiplexing (OFDM) backscatter modulation. The presented architecture performs delta-sigma modulation (DSM) on the baseband OFDM signal to shape the backscattered noise power, reducing the overall noise floor in the vicinity of the transmitted subcarriers. We experimentally demonstrated the spectral benefits of the design with a low-cost

prototype using an FPGA for the digital logic and a CMOS RF switch for the backscatter modulator. We additionally validated that synthetic sensor data (represented by a digitized sine wave) could be reliably received and decoded using an off-the-shelf software-defined radio.

The DSM used in this work has several parameters that allow a designer to trade off between in-band and out-of-band noise performance. These parameters include the oversampling rate, the gain, the comparator threshold, and the number of filter stages (i.e. the filter order) of the DSM. Since low-power backscatter communication systems are typically deployed in highly-constrained systems, it will be important to characterize the system-levels trade-offs of these parameters, for example, improving noise performance with a higher oversampling rate at the cost of increased power consumption. Further improvements could be achieved by using higher-order cascaded DSMs [7]. Normally higher-order modulators incur additional cost and digital logic complexity, however, using the hardware-efficient look-up table (LUT) architecture presented here could retain low hardware complexity.

A trade off with the DSM architecture is that it reduces the quantization noise near the subcarriers while increasing the noise out-of-band at higher frequencies. Typical DSM architectures use a low-pass filter after the DSM to reduce the out-of-band noise levels. For DSM backscatter applications, the antenna and/or analog impedance matching network(s) could act as a filter to pass the subcarriers while attenuating out-of-band noise. Future work should characterize noise suppression in over-the-air tests and whether the out-of-band noise has an appreciable effect on receiver sensitivity.

Acknowledgment

The authors would like to thank Dr. Eleftherios Kampianakis for his assistance with the receiver. This material is based upon work supported by the National Science Foundation Graduate Research Fellowship under Grant No. DGE-1762114 and the European Union's Horizon 2020 research and innovation programme under the Marie Skłodowska-Curie grant agreemnt No. 101027005.

References

[1] J. Kimionis, A. Bletsas, and J. N. Sahalos, "Increased range bistatic scatter radio," *IEEE Transactions on Communications*, vol. 62, no. 3, pp. 1091–1104, March 2014.

[2] A. Tang, Y. Kim, G. Virbila, and M. F. Chang, "A 5.8 GHz 1.77mW AFSK-OFDM CMOS backscatter transmitter for low power IoT applications," in *Proceedings of the 2018 IEEE/MTT-S International Microwave Symposium (IMS)*, June 2018, pp. 259–261.

[3] R. Correia and N. B. Carvalho, "OFDM-like high order backscatter modulation," in *2018 IEEE MTT-S International Microwave Workshop Series on 5G Hardware and Systems Technology (IMWS-5G)*, Aug. 2018, pp. 1–3.

[4] J. Rosenthal and M. S. Reynolds, "Hardware-efficient all-digital architectures for OFDM backscatter modulators," *IEEE Transactions on Microwave Theory and Techniques*, vol. 69, no. 1, pp. 803–811, Dec. 2020.

[5] T. Haque, H. Elkotby, P. Cabrol, Y. Zhang, R. Pragada, and D. Castor, "A 256-QAM backscatter transponder architecture using delta-sigma load modulation for 6G ultra-low-power IoT devices," in *Proc. IEEE 93rd Vehicular Tech. Conf. (VTC2021-Spring)*, 2021, pp. 1–7.

[6] J. Candy and G. Temes, "Oversampling methods for data conversion," in *[1991] IEEE Pacific Rim Conference on Communications, Computers and Signal Processing Conference Proceedings*, 1991, pp. 498–502 vol.2.

[7] S. Haykin, "Delta modulation," in *Communication Systems*, B. Zobrist, Ed. New York, NY, USA: John Wiley & Sons, Inc., 2001, p. 222.

[8] J. Rosenthal and M. S. Reynolds, "All-digital single sideband (SSB) Bluetooth Low Energy (BLE) backscatter with an inductor-free, digitally-tuned capacitance modulator," in *Proceedings of the 2020 IEEE/MTT-S International Microwave Symposium (IMS)*, Aug. 2020, pp. 468–471.

[9] S. J. Thomas and M. S. Reynolds, "A 96 Mbit/sec, 15.5 pJ/bit 16-QAM modulator for UHF backscatter communication," in *Proceedings of the 2012 IEEE International Conference on RFID*, Apr. 2012, pp. 185–190.

[10] S. J. Thomas, E. Wheeler, J. Teizer, and M. S. Reynolds, "Quadrature amplitude modulated backscatter in passive and semipassive UHF RFID systems," *IEEE Transactions on Microwave Theory and Techniques*, vol. 60, no. 4, pp. 1175–1182, April 2012.

[11] J. Rosenthal, A. Sharma, E. Kampianakis, and M. S. Reynolds, "A 25 Mbps, 12.4 pJ/b DQPSK backscatter data uplink for the NeuroDisc brain-computer interface," *IEEE Transactions on Biomedical Circuits and Systems*, vol. 13, no. 5, pp. 858–867, Oct. 2019.